

Source-based Multifractal Detrended Fluctuation Analysis for Discrimination of ADHD Children in a Time Reproduction Paradigm

Shiva Khoshnoud^{1,3}, Mohammad Ali Nazari² and Mousa Shamsi³

¹*Institute for Frontier Areas of Psychology and Mental Health, Freiburg, Germany*

²*Faculty of Advanced Technologies in Medicine, Iran University of Medical Sciences, Tehran, Iran*

³*Biomedical Engineering Faculty, Sahand University of Technology, Tabriz, Iran*

Keywords: Multifractal Detrended Fluctuation Analysis, ADHD, Time Perception, EEG.

Abstract: Electroencephalography recordings have a scale-invariant structure and multifractal detrended fluctuation analysis (MF-DFA) could quantify the fluctuation dynamics of these recordings in different brain states. However, the channel-based electrical activity of the brain has low spatial resolution and considering the source-level activity patterns is a good answer for this restriction. In this work, the multifractal spectrum parameters of the channel-based EEG, as well as the corresponding source-based independent components in children with Attention Deficit Hyperactivity Disorder (ADHD) and the age-matched control group, has been investigated. Considering the perceptual timing deficit in children with ADHD, for the analysis of the multifractality, two brain states including the eyes-open rest and the time reproduction condition have been considered. The results obtained showed that switching from rest to the time reproduction condition increases the degree of multifractality and so the complexity and non-uniformity of the signal. While the channel-based multifractal properties could not significantly distinguish two groups, the results for the source-based multifractal analysis showed a significantly decreased degree of multifractality for children with ADHD in prefrontal, mid-frontal and right frontal source clusters suggesting reduced activation of these clusters in this group. Utilizing support vector machine (SVM) classifier it is found that, the source-based multifractal features provide a significantly higher accuracy rate of 86.67% in comparison to the channel-based measures.

1 INTRODUCTION

Electroencephalography (EEG) recordings as a nonstationary time series possess a scale-invariant structure which indicates that signal repeats its structure on different sub-intervals (Eke, Herman, Kocsis, & Kozak, 2002; Ihlen, 2012; Zorick & Mandelkern, 2013). Time series with a complex structure like EEG are multifractal and the multifractal detrended fluctuation analysis (MF-DFA) has been proposed for evaluation of their fractal properties (Kantelhardt et al., 2002). Several reports suggest that changes in the scale-invariant structure of the biomedical signals reflect changes in the adaptability of physiological processes and successful treatment of pathological conditions might changes the fractal structure and improve health (Goldberger et al., 2002). Multifractal properties of the sleep stage EEG signals have been assessed in several studies representing that these measures correlated with the sleep depth, exhibiting

different values for deeper sleep stages (Ma, Ning, Wang, & Bian, 2006; Weiss, Clemens, Bódizs, & Halász, 2011; Weiss, Clemens, Bódizs, Vágó, & Halász, 2009; Zorick & Mandelkern, 2013). Zorick & Mandelkern (2013) revealed that even short EEG tracings represent significant dissimilarities in the width of the multifractal spectrum for the different sleep stages. Assessing the height of the multifractal spectrum, Weiss et al. (2011, 2009) indicated that EEG signals tend to be less multifractal during NREM4 compared to NREM2 and REM sleep stages. Moreover, the predictive power of multifractal parameters in epilepsy research was also examined in order to detect and predict focal seizures (Dick & Svyatogor, 2012; Dutta, Ghosh, Samanta, & Dey, 2014; Easwaramoorthy & Uthayakumar, 2010; Figliola, Serrano, & Rosso, 2007). Fractal parameters have also been utilized to study the scaling behavior of the fluctuations of the EEG while listening to musical stimuli (Maity et al., 2015; Natarajan, Acharya U, Alias, Tiboleng, &

Puthusserypady, 2004). Despite this consistent evidence for the brain-state related adaptability of the multifractal structure, a few studies have been conducted in the area of neurodevelopmental disorders. Attention-deficit hyperactivity disorder (ADHD) is a common neurodevelopmental disorder in school-aged children which exhibit varying levels of hyperactivity, inattention, and impulsivity, and substantially affect their cognitive performance (American Psychiatric Association, 2013; Sadock & Sadock, 2011).

In our previous study, the multifractal spectrum alterations of the resting-state EEG in children with ADHD have been identified (Khoshnoud, Nazari, & Shamsi, 2018). More precisely, during rest condition, over frontal and right parietal scalp channels, the multifractal spectrum was higher in children with ADHD compared to the age-matched control group. This elevated multifractal structure suggests more complex EEG patterns in children with ADHD compared to the healthy subjects during rest. Considering this outcome, an investigation of the multifractal structure of the EEG signals during different paradigms in this group would have a great impact on understanding their disorder. Several studies have demonstrated that children with ADHD have deficits in perceptual timing (Barkley, 1997; Barkley, Edwards, Laneri, Fletcher, & Metevia, 2001; Barkley, Koplowitz, Anderson, & McMurray, 1997; Noreika, Falter, & Rubia, 2013; Rubia, Halari, Christakou, & Taylor, 2009; Toplak & Tannock, 2005; Toplak, Dockstader, & Tannock, 2006). Taking into account the different cortical activity patterns of these children during time reproduction (Khoshnoud, Shamsi, Nazari, & Makeig, 2017), one could expect to see distinct multifractal structures for these cortical sources during the time reproduction condition.

To address this issue, we conducted an EEG study in children with ADHD and age-matched control subjects during two EEG recording sessions: eye-open rest and time reproduction condition. We used both the channel-based and the source-based multifractal spectrum analysis in order to visualize distinguished patterns of activity in both groups. Finally, two groups were classified based on these distinct multifractal patterns utilizing a support vector machine (SVM) classifier. Our main hypothesis was that children with ADHD would exhibit distinct multifractal structure during both EEG recording sessions and this pattern would be more distinguishable in the source-based level analysis.

2 MATERIALS AND METHODS

2.1 Participants and the Experimental Design

The EEG data used here is the authors' previously recorded dataset consisting of EEG time series of 15 ADHD and 19 controls, 7-11 years of age in the eyes-open rest and time reproduction conditions. Details about the diagnosis criteria and inclusion procedures could be found in Khoshnoud et al. (2017). EEG recording starts with the eyes-open resting period for 3 min followed by a visual time reproduction task for approximately 10 min. In each trial, following a trial start cue, a target white disk is displayed on the screen center indicating the start of a target interval of 1000 or 2200 ms (short and long encoding phase). Participants are requested to keep this interval in mind and reproduce it after a waiting period of 1500 ms as indicated by a red disk displayed at the screen center.

2.2 Data Processing

EEG data collection was accomplished using the Mitsar® amplifier with 21 channels and WinEEG® software. The reference electrodes were linked ear lobes, with the ground electrode placed on AFZ. The sampling frequency was 250 Hz. For this study, we were particularly interested in the MF-DFA analysis of the channel-based EEG signals as well as the source-based components of the signals during both recording sessions. Therefore each analysis was followed by a specific processing procedure. The EEG data were processed using EEGLAB functions (version 13) (Delorme & Makeig, 2004) running on Matlab (MATLAB2013a, The Mathworks, Inc.).

At first, the raw EEG signals were high-pass filtered above 1 Hz and were low-pass filtered below 50 Hz using a windowed FIR sync filter to remove line noise and other artifacts. After re-referencing to a common average reference, the EEG time series were visually inspected to reject periods with abnormally high artifact levels. After this general pre-processing step, the channel-based study was continued with the MF-DFA analysis (section 2.3). For the source-based study, additional processing steps have been performed. The schematic overview of these steps has been illustrated in Figure 1. At first, the raw EEG signals were high-pass filtered above 1 Hz and were low-pass filtered below 50 Hz using a windowed FIR sync filter to remove line noise and other artifacts.

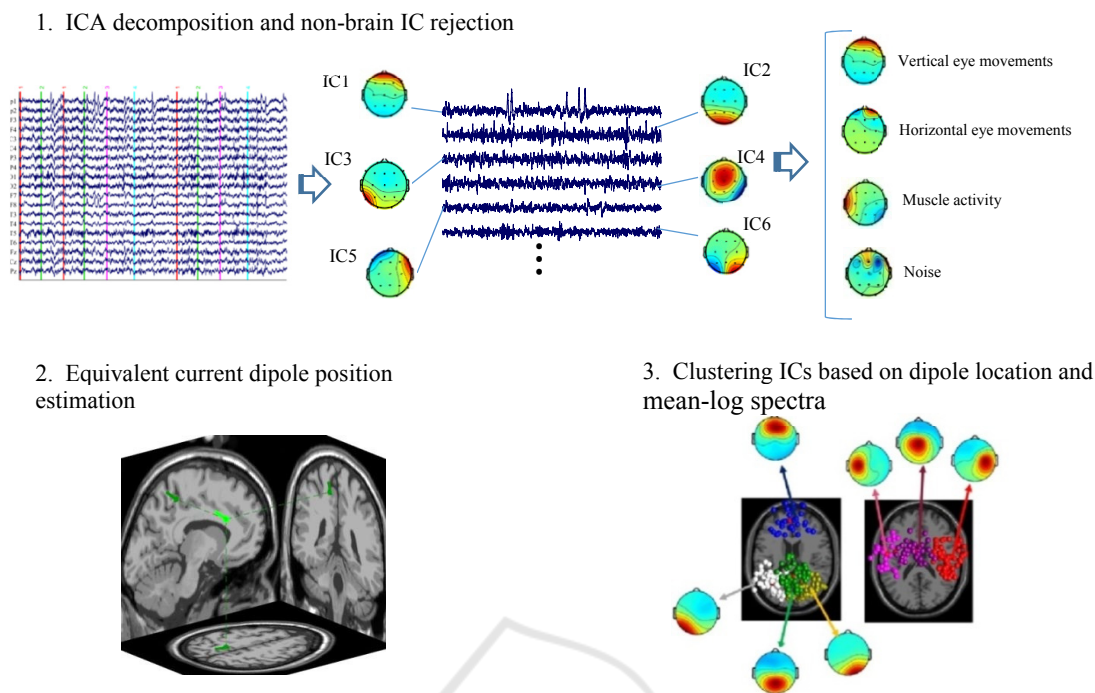


Figure 1: Overview of the EEG data processing steps for the source-based MF-DFA analysis after pre-processing of the data. 1) Single-subject EEG data are decomposed by AMICA into a set of ICs and then nonbrain ICs are identified and removed from further processing. 2) Equivalent current dipole positions for resumed ICs are estimated. 3) Based on the dipole position and mean log spectra, the ICs are clustered across subjects into 7 clusters.

After re-referencing to a common average reference, the EEG time series were visually inspected to reject periods with abnormally high artifact levels. After this general pre-processing step, the channel-based study was continued with the MF-DFA analysis (section 2.3). For the source-based study, additional processing steps have been performed. The schematic overview of these steps has been illustrated in Figure 1.

ICA Decomposition- In order to decompose the pre-processed EEG data to a corresponding set of statistically independent source components, the Adaptive Mixture Independent Component Analysis (AMICA) algorithm (Palmer, Kreutz-Delgado, & Makeig, 2006, 2011; Palmer, Makeig, Kreutz-Delgado, & Rao, 2008) was used. AMICA has been shown to have superior performance among blind source separation algorithms for EEG decomposition (Delorme, Palmer, Onton, Oostenveld, & Makeig, 2012). After identifying and removing the eye and muscle activity-related components based on their spectra, scalp maps, and time courses, the brain-related independent components (ICs) were selected for further analysis (Makeig et al., 2002).

Equivalent Current Dipole Position Estimation-

Subsequently, equivalent source distribution of the brain-related ICs were computed using the DIPFIT toolbox within EEGLAB (http://sccn.ucsd.edu/wiki/A08:_DIPFIT). Scalp electrode positions were co-registered to an MNI template brain (Montreal Neurological Institute, MNI, and Quebec) using nonlinear warping. Then, a best-fitting equivalent current dipole was matched to each IC using a template three-shell boundary element method (BEM) head model based on the MNI brain template. ICs with the equivalent dipole model located within the brain which explained more than 90% of the variance of the IC scalp map were retained for further analysis.

IC Clustering-

ICs across subjects were classified based on similarities in IC dipole locations and mean log spectra using K-means algorithm and totally seven clusters were computed (Makeig et al., 2002; Onton & Makeig, 2006). ICs whose distance to any cluster centroid was more than three standard deviations from the cluster mean distance were considered outliers.

2.3 Multi-fractal Detrended Fluctuation Analysis

There are two distinct types of multifractality in time series: multifractality due to a broad probability density function and multifractality due to long-range correlations of the small and large fluctuations in time series. While the former cannot be removed by shuffling the data, the corresponding shuffled series of the latter one will exhibit no- or weaker multifractality scaling behavior (Kantelhardt et al., 2002). The complete procedure for Mf-DFA is divided into the following steps:

Step 1: The noise-like structure of the time series x_k with length N was converted into a random walk:

$$Y(i) = \sum_{k=1}^i [x_k - \langle x \rangle], \quad i = 1, \dots, N \quad (1)$$

Step 2: The integrated time series are divided into N_s number of non-overlapping segments with equal lengths s as follows:

$$N_s = \text{int}(N/s) \quad (2)$$

Step 3: For each segment, the root mean square (RMS) variance is calculated by Equation (3), in which $v = N_s + 1, \dots, 2N_s$ and $y_v(i)$ is the fitting polynomial in segment v :

$$F^2(s, v) \equiv \frac{1}{s} \sum_{i=1}^s \{Y[N - (v - N_s)s + i] - y_v(i)\}^2 \quad (3)$$

Step 4: Subsequently, to obtain the q th-order fluctuation function, the mean RMS value over all segments is calculated:

$$F_q(s) \equiv \left\{ \frac{1}{2N_s} \sum_{v=1}^{2N_s} [F^2(s, v)]^{q/2} \right\}^{1/q} \quad (4)$$

Step 5: Because of spatial and temporal variations in the scale-invariant structure of the multifractal time series, the procedure is repeated for several time scales (s). Finally, the scaling behavior of the fluctuation functions is determined by analyzing the log-log plots of $F_q(s)$ versus s for each value of q :

$$F_q(s) \approx s^{h(q)} \quad (5)$$

The q -order Hurst exponent is related to the scaling exponents $\tau(q)$ by Equation (6):

$$\tau(q) = qh(q) - 1 \quad (6)$$

Thereafter, scaling exponents could be converted into the q -order singularity exponent (α) and the q -order singularity dimension ($f(\alpha)$) by the following equations to obtain the multifractal singularity spectrum:

$$\alpha = \tau'(q) \quad \text{and} \quad f(\alpha) = q\alpha - \tau(q) \quad (7)$$

The width and shape of the multifractal spectrum are valuable factors for distinguishing different multifractal structures. In this study, we used the width ($d\alpha = \max \alpha - \min \alpha$) and the height of the spectrum ($df(\alpha) = \max f(\alpha) - \min f(\alpha)$) as well as mean (α) and mean $f(\alpha)$ to evaluate the multifractal spectrum.

2.4 Classification

The distinguishability of the extracted fractal features was examined using a support vector machine algorithm. The aim of the SVM is to compute an optimal separating hyperplane to which the distance from each nearest data sample in each class is maximized (Vapnik & Lerner, 1963). SVM offers a solution for non-separable cases, using kernel mapping with projecting the data into a higher-dimensional feature space using a nonlinear function ($\phi(\cdot)$). Given a weight vector W and a bias term b , the formulation of the hyperplane is as follows:

$$W^t \phi(\cdot) + b = 0 \quad (8)$$

To find such an optimum hyperplane, the optimization problem is as follows:

$$\text{Minimize } J(W) = \frac{1}{2} \|W\|^2 \quad (9)$$

$$\text{Subject to } d_i(W^T \phi(x) + b) \geq 1$$

The above-mentioned problem is solved using the Lagrangian optimization theory. Here, we tested linear, polynomial and RBF kernel functions and RBF kernel led to a better discrimination accuracy.

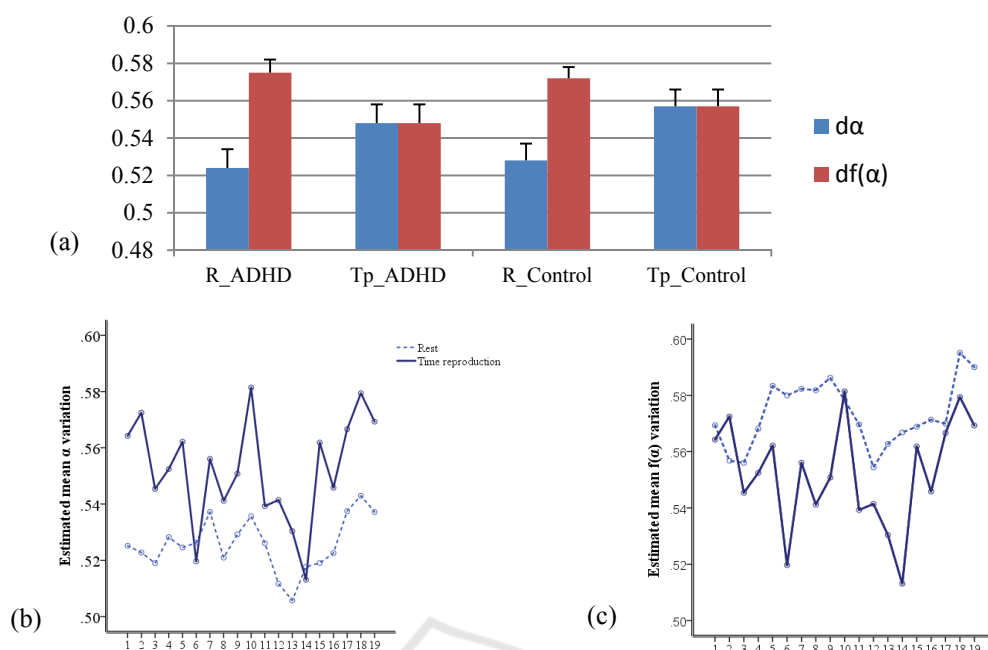


Figure 2: a) Average values of the width ($d\alpha$) and height ($df(\alpha)$) of the channel-based multifractal spectrum in children with ADHD and age-matched controls during rest (R) and time reproduction (Tp). b) Mean $d\alpha$ for all scalp electrodes during rest and time reproduction. c) Mean $df(\alpha)$ for all scalp electrodes during rest and time reproduction.

3 RESULTS

3.1 Group Differences in the Channel-based MF-DFA

As mentioned in the previous section, the EEG time series have multifractal structures that contain both types of multifractality. The important intellectual question here is how this multifractality changes through different brain states. In order to assess variations in the degree of multifractality in transition from the rest to time reproduction, average MF spectra for each EEG signal in both conditions (rest and time reproduction) were computed. A comparison of the multifractal structures in the two brain states was made by evaluating four features extracted from MF spectra in each time series for all subjects. These features are as follows: the width ($d\alpha$) and the height ($df(\alpha)$) of the spectrum, mean q-order singularity exponent ($mean_\alpha$), and mean q-order singularity dimension ($mean_f(\alpha)$). Repeated measures analysis of variance (ANOVA) was conducted separately on each feature with the condition (rest vs. time reproduction) and electrode positions as the within-subject factors and group (ADHD vs. control) as the between-subject factor. For the width and the height features, ANOVA

revealed a significant main effect of condition [(F (1, 32) = 9.15; p = .005), (F (1, 32) = 8.45; p = .007)], demonstrating that for both groups, the shape of the multifractal spectrum in the two conditions differ significantly. In transition from the rest to time reproduction, the width increased and the height decreased. Figure 2 (a) shows the averaged values of these two extracted features along with the standard deviations of them in each condition for both groups. Also, the electrode \times condition interaction effect was significant. Figure 2(b) and 2(c) demonstrate the significant rise in the width and significant decline in the height of the multifractal spectrum during time reproduction in most of the scalp electrodes. For $mean_f(\alpha)$, there was a significant effect of condition (F (1, 32) = 8.52; p = .006) showing lower values for time reproduction than rest state (Figure 3(a)). The effect of the group just for the $mean_\alpha$ was near significant (F (1, 32) = 8.45; p = 0.07) with controls showing higher values than ADHD subjects regardless of the paradigm (Figure 3(b) and 3(c)). This lower mean q-order singularity exponent value in individuals with ADHD shows that the degree of multifractality in signals of this group is marginally lower than control subjects.

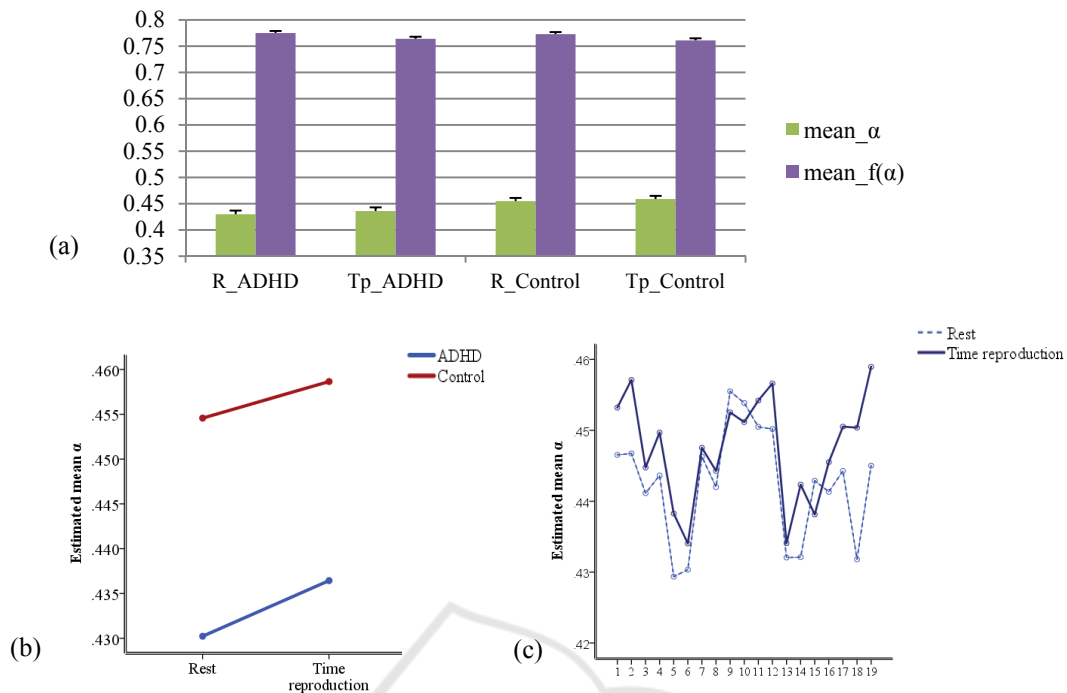


Figure 3: a) Average values of the q -order singularity exponent (mean_α) and q -order singularity dimension ($\text{mean}_f(\alpha)$) of the channel-based multifractal spectrum in children with ADHD and age-matched controls during rest (R) and time reproduction (Tp). b) mean_α for children with ADHD and control in transition from rest to time reproduction. c) mean_α for all scalp electrodes during rest and time reproduction.

3.2 Group Differences in the Source-based MF-DFA

The channel-based multifractal features showed significant alterations between two conditions, failed to clearly distinguish two groups. Concerning better spatial resolution of the source-based analysis, one could expect to see a more significant trend in the source components. However, unlike scalp channels, a pair of independent components from two subjects might resemble or differ from each other in many ways. Even with one subject in a different paradigm, the results could be different as each paradigm leads to specific source components. Therefore making direct comparisons about the transition from rest to the time reproduction for ICs would not be logical. Notwithstanding, it is possible to assess ICs' multifractal properties for two groups during one paradigm. To achieve this, the multifractal spectrum of 349 ICs from 34 subjects in 7 clusters were calculated and averaged for each group and each cluster. Figure 4(a) represents the clusters including two occipital, one occipital-temporal, three frontal, and one prefrontal cluster. The averaged multifractal spectrums of each cluster for both groups during the encoding phase of the time reproduction task has

been shown in figure 4(b). According to the figure 4(b), in the prefrontal, mid-frontal and right frontal clusters, the multifractal spectrum of subjects with ADHD in both durations exhibited a leftward shift reflecting a lower degree of multifractality for these individuals in these clusters. Similar to the previous section, for the purpose of statistical analysis four features of these spectrums ($d\alpha$, $f(\alpha)$, mean_α , and $\text{mean}_f(\alpha)$) were assessed utilizing independent t-test. The results showed that mean_α for the prefrontal, mid-frontal and right frontal source clusters in the ADHD group were significantly lower than that of the control group for both durations (p -values < 0.02). Moreover, $\text{mean}_f(\alpha)$ for the right occipital cluster in individuals with ADHD was significantly higher than that for control subjects (p -value < 0.019). Multifractal spectrum width in the prefrontal cluster also displayed a significant difference between two groups with the lower value for the ADHD group than controls.

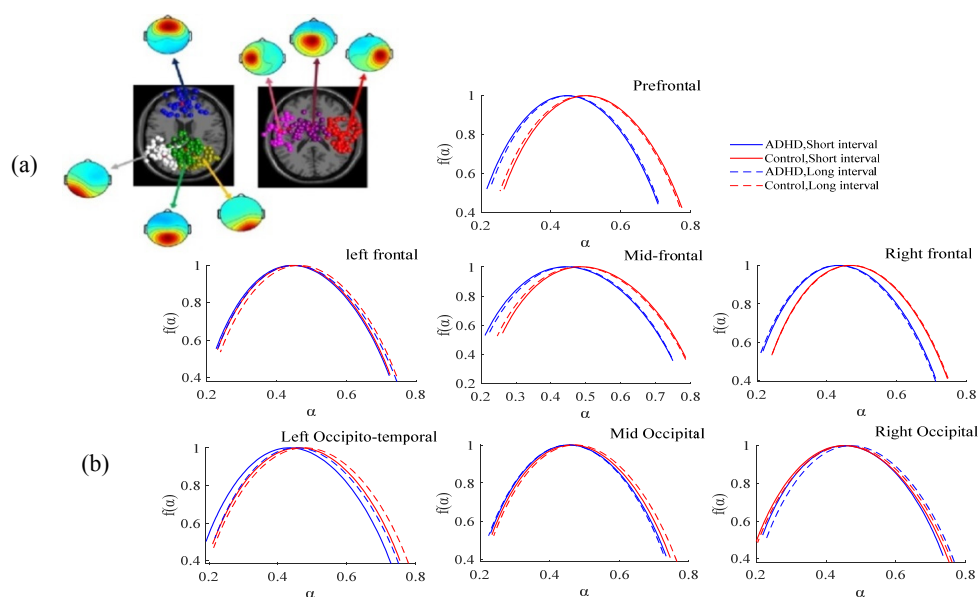


Figure 4: a) 7 IC source clusters including two occipital, one occipital-temporal, three frontal, and one prefrontal cluster. b) Averaged multifractal spectrums of each source cluster for each group (ADHD vs. control) during two interval reproduction (short vs. long).

3.3 Classification Results for the Both Channel-based and Source-based Features

The multifractal features ability to distinguish between two groups was furthermore evaluated by passing them to the SVM classifier. For both the channel-based and the source-based measures, SVM with three types of kernel functions (linear, polynomial, and radial basis functions (RBF)) were tested. Here, the results for the RBF SVM are mentioned as it yielded better results. Using the holdout cross-validation method, 80% of the data were used to train the classifiers; the other 20% were kept for testing and the results were reported as an average accuracy after 20 repetitions.

Channel-based Classification- In favor of data reduction, the 76 channel-based multifractal features (19 electrode * 4 features) were reduced to the 15 principle components using the principle component analysis preserving 90% of the signal variance. Afterward, these principal components were fed into the SVM classifier. Table 1 summarizes the results of applying multifractal features to the SVM. Using channel-based multifractal features showed 73.5% and 77.78% accuracy during rest and time reproduction, respectively. This outcome revealed an increase in the accuracy of the classification of two groups applying the time reproduction paradigm.

Source-based Classification- as reflected by the group discrepancy results in section C, $mean_ \alpha$, and $mean_ f(\alpha)$ parameters yielded significant differences across the two groups. Hence, these two features were chosen for the classification with the SVM. Considering the ICA algorithm, some subjects might not have an IC in a cluster. In this case, the nearest dipole to the central dipole of that cluster was identified and the above mentioned multifractal features from the corresponding IC were considered as the features of that cluster for that subject. Fourteen features (7 clusters * 2 features) for each subject were passed to the SVM classifier with the holdout cross-validation method described above. The results have been reported in Table 1. The $mean_ \alpha$ and the $mean_ f(\alpha)$ presented high accuracy values of 86.67% and 81.67%, respectively. It is in accordance with the previous results in section C that $mean_ \alpha$ showed the most distinguishing feature between the two groups.

4 DISCUSSION

In the current study, we used multifractal properties to describe the dynamics of brain electrical activity during two different brain states, the eyes-open rest and the time reproduction condition. Furthermore, multifractal features were assessed in the channel-based as well as the source-based level to discover

group discrepancies between ADHD and age-matched control participants. We found evidence of multifractal structures as well as the presence of both types of multifractality in the EEG signals. This confirmed the presence of the scale-invariant structure in the brain activity as stated in the previous studies (Ihlen, 2012; Zorick & Mandelkern, 2013). Interestingly, the channel-based assessment revealed that the shape of the multifractal spectrum exhibited a significant alteration from rest to the time reproduction condition. According to our statistical results, in transition from the rest to time reproduction, the width of the multifractal spectrum increased and its height decreased significantly for both groups. This indicates that switching from rest state to the time reproduction state increased the degree of multifractality of the EEG signals in both groups. As represented in Figure 2(b-c), this trend has been seen in almost all studied scalp electrode sites.

The rise of the width of the singularity spectrum during the time reproduction demonstrates an increase of the non-uniformity and the complexity of the signal and, hence, a climb in the degree of the multifractality. An increase in brain complexity can be regarded to be a measure for the brain reaching an active state (Maity et al., 2015). According to the MF-DFA, this increase is due to the rise in the values of the q-order singularity exponents, hence increase in the weak variations of the signal ($h > 0$ for $q < 0$) since at large variations ($q < 0$) signals behavior become more monofractal (Kantelhardt et al., 2002). This can be interpreted in the light of more beta activity during time perception. Beta oscillations have been reported to correlate with time perception (Ghaderi et al., 2018; Kononowicz & Rijn, 2015).

Similarly, a decline in the q-order singularity dimension variation and mean ($df(\alpha)$ and $mean_f(\alpha)$) reflected a higher degree of multifractality for EEG time series during time reproduction. This outcome confirmed the previous studies arguing the applicability of the scale-invariant or multifractal structures to reflect changes in the brain states (Dick, Svyatogor, Ishinova, & Nozdrachev, 2012; Dutta et al., 2014; Figliola et al., 2007; Ma et al., 2006; Maity et al., 2015; Natarajan

et al., 2004; Weiss et al., 2011, 2009; Zorick & Mandelkern, 2013). Maity et al. (2015) reported a considerable increase in alpha and theta multifractal spectrum width and hence complexity of these particular brain waves when subjects listen to the Tanpura drone. Although channel-based multifractal features provide significant measures for distinguishing between the rest and the time reproduction brain states, they showed weak results for differentiating the two groups. Among the multifractal properties, just the mean q-order singularity exponent displayed near significant lower values for ADHD subjects compared with controls. In both conditions the mean α , hence the degree of multifractality of EEG signals for ADHD group was lower than that for healthy control subjects.

It is well known that EEG has a limited spatial resolution and the channel-level analysis can only provide limited information about the cortical regions involved in the generation and the perturbation of these cortical regions activity (Makeig, Bell, Jung, & Sejnowski, 1996). One possible solution for improving the spatial resolution of EEG is to perform source analysis by means of source localization methods. To our knowledge, this is the first time that MF-DFA is performed on the source ICs of the EEG signals. Our main hypothesis was that children with ADHD would exhibit distinct multifractal structure during both EEG recording conditions and this pattern is more distinguishable in the source-based analysis. Our source-based multifractal analysis in the time reproduction task revealed significant differences between two groups reaching better spatial resolution. As stated in the results section, the prefrontal, mid-frontal and right frontal clusters displayed a significantly different multifractal spectrum shape for both short and long duration reproduction conditions for both groups. To be more precise, the multifractal spectrum of individuals with ADHD exhibited a leftward shift which reflects lower degree of multifractality, consequently, less complexity and more uniformity of ICs in these individuals compared to the control subjects. The central tendency of the multifractal spectrum is closely related to the monofractal Hurst exponent.

Table 1: Classification accuracy for the channel-based and the source-based multifractal features.

Features	The channel-based features	The source-based features	
		Mean- α	Mean $f(\alpha)$
Rest	73.5%	-----	-----
Time reproduction	77.78%	86.67%	81.67%

The central tendency between 0.5-1 reflects a time series with long-range correlations and below 0.5 would be an index of anti-correlated structure (Kantelhardt et al., 2002). Therefore the leftward shift in the multifractal spectrum of participants with ADHD indicates less long-range correlations in their EEG signals. This suggests that IC time series in participants with ADHD in prefrontal, mid-frontal, and right frontal regions are more uniform and regular than in the control group. Similarly, it might be because of fewer small and large variations on the time series in these areas. These results are in line with the previous studies reporting reduced activation in the right dorsolateral prefrontal cortex (DLPFC) and supplementary motor area (SMA) in individuals with ADHD during a time discrimination task (Rubia et al., 2009; Smith, Taylor, Brammer, Halari, & Rubia, 2008). Correspondingly, in our previous study, the higher amplitude of the mid-frontal P300 evoked by the onset of the encoding phase of time reproduction for ADHD individuals has been linked to inappropriate and insufficient allocation of attentional resources for the encoding of the target interval (Khoshnoud et al. 2017).

Both groups of features were separately exploited for the classification with SVM. While the best accuracy for the 4 channel-based multifractal features was during time reproduction condition with 77.78%, the source-based mean α displayed a significantly higher accuracy with 86.67%. Using the source-based multifractal features not only increased the accuracy rate but also reduced the number of features from 76 ($19 * 4$) to 14 ($7 * 2$) for each participant. Our results confirmed our main hypothesis by showing greater distinguishability of the source-based multifractal features. Nevertheless, the present study has some limitations that should be considered. First and foremost is that this study utilized a clinical EEG recording system with 19 electrodes, which resulted in a limited set of ICs and therefore restricted source clusters. We believed that using high-resolution EEG signals will lead to more accurate source localization and subsequently more ICs which would lead to better classification accuracy. The second shortcoming of this work is the small sample size (15 ADHD and 19 controls) which might be the main source of low statistical power for discrepancies between the two groups.

5 CONCLUSIONS

This study conducted a multifractal detrended fluctuation analysis on the neural activities of the

brain in individuals with ADHD and age-matched healthy children during the eyes-open rest and time reproduction conditions. It was found that multifractality could quantify the fluctuation dynamics from two different pathological EEGs taken at these two conditions. The results showed that the sensor-level and the source-level multifractal features provide different information about the brain state. According to the results, in transition from the rest to the time reproduction, the degree of multifractality of the EEG signals for both groups displayed a significant increase indicating more complex and non-uniform activity during time reproduction. Also, the prefrontal, mid-frontal and right frontal clusters displayed significantly different multifractal spectrum shapes for both groups. Independent components in these clusters for participants with ADHD exhibited less long-range correlations suggesting reduced activation in these source regions.

ACKNOWLEDGEMENTS

The first author would like to thank Dr. Marc Wittmann and Dr. Scott Makeig for their support and their great comments on this project.

REFERENCES

- American Psychiatric Association. (2013). *Diagnostic and statistical manual of mental disorders (DSM-5®)*. American Psychiatric Pub.
- Barkley, R. A. (1997). Attention-deficit/hyperactivity disorder, self-regulation, and time: Toward a more comprehensive theory. *Journal of Developmental & Behavioral Pediatrics, 18*(4), 271–279.
- Barkley, R. A., Edwards, G., Laneri, M., Fletcher, K., & Metevia, L. (2001). Executive functioning, temporal discounting, and sense of time in adolescents with attention deficit hyperactivity disorder (ADHD) and oppositional defiant disorder (ODD). *Journal of Abnormal Child Psychology, 29*(6), 541–556. <https://doi.org/10.1023/a:1012233310098>
- Barkley, R. A., Koplowitz, S., Anderson, T., & McMurray, M. B. (1997). Sense of time in children with ADHD: Effects of duration, distraction, and stimulant medication. *Journal of the International Neuropsychological Society, 3*(04), 359–369.
- Delorme, A., & Makeig, S. (2004). EEGLAB: An open source toolbox for analysis of single-trial EEG dynamics including independent component analysis. *Journal of Neuroscience Methods, 134*(1), 9–21. <https://doi.org/10.1016/j.jneumeth.2003.10.009>

- Delorme, A., Palmer, J., Onton, J., Oostenveld, R., & Makeig, S. (2012). Independent EEG sources are dipolar. *PLoS ONE*, *7*(2). <https://doi.org/10.1371/journal.pone.0030135>
- Dick, O. E., & Svyatogor, I. A. (2012). Potentialities of the wavelet and multifractal techniques to evaluate changes in the functional state of the human brain. *Neurocomputing*, *82*, 207–215. <https://doi.org/10.1016/j.neucom.2011.11.013>
- Dick, O. E., Svyatogor, I. A., Ishinova, V. A., & Nozdrachev, A. D. (2012). Fractal characteristics of the functional state of the brain in patients with anxious phobic disorders. *Human Physiology*, *38*(3), 249–254. <https://doi.org/10.1134/S036211971202003X>
- Dutta, S., Ghosh, D., Samanta, S., & Dey, S. (2014). Multifractal parameters as an indication of different physiological and pathological states of the human brain. *Physica A: Statistical Mechanics and Its Applications*, *396*, 155–163. <https://doi.org/10.1016/j.physa.2013.11.014>
- Easwaramoorthy, D., & Uthayakumar, R. (2010). Analysis of biomedical EEG signals using Wavelet Transforms and Multifractal Analysis. *Communication Control and Computing Technologies (ICCCCT), 2010 IEEE International Conference On*. <https://doi.org/10.1109/ICCCCT.2010.5670780>
- Eke, A., Herman, P., Kocsis, L., & Kozak, L. R. (2002). Fractal characterization of complexity in temporal physiological signals. *Physiological Measurement*, *23*(1). <https://doi.org/10.1088/0967-3334/23/1/201>
- Figliola, A., Serrano, E., & Rosso, O. A. (2007). *Multifractal detrended fluctuation analysis of tonic-clonic epileptic seizures*. *123*, 117–123. <https://doi.org/10.1140/epjst/e2007-00079-9>
- Ghaderi, A. H., Moradkhani, S., Haghighatfard, A., Akrami, F., Khayyer, Z., & Balci, F. (2018). Time estimation and beta segregation: An EEG study and graph theoretical approach. *PLoS ONE*, *13*(4), 1–16. <https://doi.org/10.1371/journal.pone.0195380>
- Goldberger, A. L., Amaral, L. A. N., Hausdorff, J. M., Ivanov, P. C., Peng, C.-K., & Stanley, H. E. (2002). Fractal dynamics in physiology: Alterations with disease and aging. *Proceedings of the National Academy of Sciences*, *99*(Supplement 1), 2466–2472. <https://doi.org/10.1073/pnas.012579499>
- Ihlen, E. A. F. (2012). Introduction to multifractal detrended fluctuation analysis in Matlab. *Frontiers in Physiology*, *3* JUN(June), 1–18. <https://doi.org/10.3389/fphys.2012.00141>
- Kantelhardt, J. W., Zschiegner, S. a., Koscielny-Bunde, E., Havlin, S., Bunde, A., Stanley, H. E., ... Stanley, H. E. (2002). Multifractal detrended fluctuation analysis of nonstationary time series. *Physica A: Statistical Mechanics and Its Applications*, *316*(1), 87–114. [https://doi.org/10.1016/S0378-4371\(02\)01383-3](https://doi.org/10.1016/S0378-4371(02)01383-3)
- Khoshnoud, S., Nazari, M. A., & Shamsi, M. (2018). Functional brain dynamic analysis of ADHD and control children using nonlinear dynamical features of EEG signals. *Journal of Integrative Neuroscience*, *17*(1), 17–30. <https://doi.org/10.3233/JIN-170033>
- Khoshnoud, S., Shamsi, M., Nazari, M. A., & Makeig, S. (2017). Different cortical source activation patterns in children with attention deficit hyperactivity disorder during a time reproduction task. *Journal of Clinical and Experimental Neuropsychology*, *40*(7), 633–649. <https://doi.org/10.1080/13803395.2017.1406897>
- Kononowicz, T. W., & Rijn, H. van. (2015). Single trial beta oscillations index time estimation. *Neuropsychologia*, *75*, 381–389. <https://doi.org/10.1016/j.neuropsychologia.2015.06.014>
- Ma, Q., Ning, X., Wang, J., & Bian, C. (2006). A new measure to characterize multifractality of sleep electroencephalogram. *Chinese Science Bulletin*, *51*(24), 3059–3064. <https://doi.org/10.1007/s11434-006-2213-y>
- Maity, A. K., Pratihari, R., Mitra, A., Dey, S., Agrawal, V., Sanyal, S., ... Ghosh, D. (2015). Multifractal Detrended Fluctuation Analysis of alpha and theta EEG rhythms with musical stimuli. *Chaos, Solitons and Fractals*, *81*, 52–67. <https://doi.org/10.1016/j.chaos.2015.08.016>
- Makeig, S., Bell, A. J., Jung, T.-P., & Sejnowski, T. J. (1996). Independent component analysis of electroencephalographic data. *Advances in Neural Information Processing Systems*, 145–151.
- Makeig, S., Westerfield, M., Jung, T.-P., Enghoff, S., Townsend, J., Courchesne, E., & Sejnowski, T. J. (2002). Dynamic Brain Sources Visual Evoked Response. *Science*, *295*(January), 690–694.
- Natarajan, K., Acharya U, R., Alias, F., Tiboleng, T., & Puthusserypady, S. K. (2004). Nonlinear analysis of EEG signals at different mental states. *Biomedical Engineering Online*, *3*(1), 7. <https://doi.org/10.1186/1475-925X-3-7>
- Noreika, V., Falter, C. M., & Rubia, K. (2013). Timing deficits in attention-deficit/hyperactivity disorder (ADHD): Evidence from neurocognitive and neuroimaging studies. *Neuropsychologia*, *51*(2), 235–266. <https://doi.org/10.1016/j.neuropsychologia.2012.09.036>
- Onton, J., & Makeig, S. (2006). Chapter 7 Information-based modeling of event-related brain dynamics. *Progress in Brain Research*, *159*, 99–120. [https://doi.org/10.1016/S0079-6123\(06\)59007-7](https://doi.org/10.1016/S0079-6123(06)59007-7)
- Palmer, J. A., Kreutz-Delgado, K., & Makeig, S. (2006). Super-Gaussian mixture source model for ICA. *Lecture Notes in Computer Science (Including Subseries Lecture Notes in Artificial Intelligence and Lecture Notes in Bioinformatics)*, *3889 LNCS*, 854–861. https://doi.org/10.1007/11679363_106
- Palmer, J. A., Kreutz-Delgado, K., & Makeig, S. (2011). *AMICA: An adaptive mixture of independent component analyzers with shared components*. San Diego, CA: Technical report, Swartz Center for Computational Neuroscience.
- Palmer, J. A., Makeig, S., Kreutz-Delgado, K., & Rao, B. D. (2008). Newton method for the ICA mixture model.

- IEEE International Conference on Acoustics, Speech and Signal Processing, 2008.*, 1805–1808. IEEE.
- Rubia, K., Halari, R., Christakou, A., & Taylor, E. (2009). Impulsiveness as a timing disturbance: neurocognitive abnormalities in attention-deficit hyperactivity disorder during temporal processes and normalization with methylphenidate. *Philosophical Transactions of the Royal Society of London B: Biological Sciences*, 364(1525), 1919–1931.
- Sadock, B. J., & Sadock, V. A. (2011). *Kaplan and Sadock's synopsis of psychiatry: Behavioral sciences/clinical psychiatry*. Lippincott Williams & Wilkins.
- Smith, A. B., Taylor, E., Brammer, M., Halari, R., & Rubia, K. (2008). Reduced activation in right lateral prefrontal cortex and anterior cingulate gyrus in medication-naïve adolescents with attention deficit hyperactivity disorder during time discrimination. *Journal of Child Psychology and Psychiatry*, 49(9), 977–985.
- Toplak, M. ., & Tannock, R. (2005). Tapping and anticipation performance in attention deficit hyperactivity disorder. *Perceptual and Motor Skills*, 100(3), 659–675. <https://doi.org/10.2466/PMS.100.3.659-675>
- Toplak, M. E., Dockstader, C., & Tannock, R. (2006). Temporal information processing in ADHD: Findings to date and new methods. *Journal of Neuroscience Methods*, 151(1), 15–29. <https://doi.org/10.1016/j.jneumeth.2005.09.018>
- Vapnik, V. N., & Lerner, A. Y. (1963). Recognition of Patterns with help of Generalized Portraits. *Avtomat. i Telemekh*, 24(6), 774–780.
- Weiss, B., Clemens, Z., Bódizs, R., & Halász, P. (2011). Comparison of fractal and power spectral EEG features: Effects of topography and sleep stages. *Brain Research Bulletin*, 84(6), 359–375. <https://doi.org/10.1016/j.brainresbull.2010.12.005>
- Weiss, B., Clemens, Z., Bódizs, R., Vágó, Z., & Halász, P. (2009). Spatio-temporal analysis of monofractal and multifractal properties of the human sleep EEG. *Journal of Neuroscience Methods*, 185(1), 116–124. <https://doi.org/10.1016/j.jneumeth.2009.07.027>
- Zorick, T., & Mandelkern, M. A. (2013). Multifractal Detrended Fluctuation Analysis of Human EEG: Preliminary Investigation and Comparison with the Wavelet Transform Modulus Maxima Technique. *PLoS ONE*, 8(7), 1–7. <https://doi.org/10.1371/journal.pone.0068360>